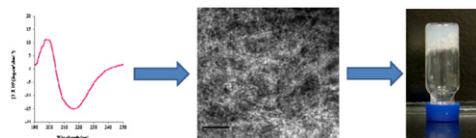# Structure and hydrogel formation studies on homologs of a lactoglobulin-derived peptide

Marie-Michèle Guy, Normand Voyer *

*PROTEO, Quebec Research Network on Protein Structure, Function and Engineering, and Département de chimie, Université Laval, Quebec City, QC, Canada, G1V 0A6*

## GRAPHICAL ABSTRACT



## ARTICLE INFO

## ABSTRACT

In order to study the impact of the amino acid sequence on the morphology of peptide-based nanostructures and their hydrogel formation, we designed a series of analogs of a milk-derived octapeptide (OP), mainly using strategic amino acid substitutions. Electronic transmission microscopy (TEM) and circular dichroism (CD) spectropolarimetry were used to analyze the nanostructures formed, and to characterize some structural features of the modified peptides. Further, the potential to form hydrogels was investigated for all of the analogous peptides. We learned that those able to undergo secondary structure transition to β-sheet conformation form strong gels. The results reported highlight some key structural properties that explain the self-assembly propensity of Peptide OP.

## 1. Introduction

Molecular self-assembly is ubiquitous in biological systems and consists of a spontaneous association of several individual entities into a coherent organization without external instructions. Recreating such phenomena artificially in controlled conditions has been the subject of intense research in the past decades [1–5]. The self-assembly of biomolecules such as peptides and proteins has significant implications in the biomedical sciences, materials research, and nanotechnology [6–13].

In peptide self-assembly, the initiation step is often the association of peptide units into β-sheets [14–20]. The establishment of noncovalent molecular interactions, including van der Waals, electrostatic, and hydrophobic interactions, as well as hydrogen bonding, allow the grouping and stabilization of several β-sheets together, which ultimately results in supramolecular structure formation.

Several reports have described the formation of different nanostructures, such as nanotubes, nanofibers, and hydrogels, from self-assembling peptides [9,10,13,14,16,20–25]. Peptide hydrogels are highly hydrated materials resulting from peptide nanofibers entangled together in a three-dimensional network that entraps a large amount of water molecules; this leads to gel formation [25,26]. Prospective applications of hydrogels made from β-sheet fibrillar networks include matrices for the separation of large biomolecules (such as proteins), scaffolds for cell growth and tissue engineering, encapsulation and controlled release of drugs and bioactive molecules, and templates for mineral growth [27–29]. Many factors influence the behavior of peptide self-assembly, including the amino acid sequence, concentration, pH, temperature, solvent composition, and ionic strength [30–34]. The preparation of materials via peptide self-assembly, employing both careful design of the individual molecules and selection of appropriate physico-chemical conditions, allows one to define ultimate material properties such as chemical functionality, material morphology, and mechanical and viscoelastic properties [13,20].

* Corresponding author. Tel.: +1 418 656 3613; fax: +1 418 656 7916.
*E-mail address:* Normand.Voyer@chm.ulaval.ca (N. Voyer).

**Table 1**
Homologs used and their modification compared to the parent OP.

| Parameter | Sequence | # | Modification |
|---|---|---|---|
| Original milk peptide | L I V T Q T M K | OP | |
| Hydrophobic/Hydrophilic Ratio | G I V T Q T M K | H1 | Decrease *N*-terminal hydrophobicity |
| | L L I V T Q T M K | H2 | Increase *N*-terminal hydrophobicity |
| | L I V T Q T M A | H3 | Decrease *C*-terminal hydrophilicity/Remove one + charge |
| | L I V T Q T K K | H4 | Increase *C*-terminal hydrophilicity/Add one + charge |
| | L L I V T Q T K K | H5 | Extend both extremities/Add one + charge |
| Lysine substitution (*C*-terminal extremity) | L I V T Q T M R | L1 | Change side chain pKa |
| | L I V T Q T M E | L2 | Change side chain charge |
| Charge distribution | Ac L I V T Q T M K | D1 | Block *N*-terminal extremity/Decrease overall + charge |
| | L I V T Q T M K NH2 | D2 | Block *C*-terminal extremity/Increase overall + charge |
| | K M T Q T V I L | D3 | Sequence inversion/Invert charge distribution |

Our group focused on the self-assembly of an octapeptide derived from the milk protein β-lactoglobulin, called Peptide OP (Table 1), which undergoes self-assembly by a secondary structure transition to β-sheet conformation in a solution at basic pH [35]. Peptide OP with an amino acid sequence LIVTQTMK is amphiphilic, with a hydrophobic part located at the N-terminal extremity and a hydrophilic lysine residue at the C-terminal extremity. Previous work revealed that Peptide OP self-assembly and hydrogel formation can be triggered significantly by pH and peptide concentration variation, whereas temperature and ionic strength variations have little influence on these processes [36]. On that basis, we proposed that the self-assembly of Peptide OP is driven by β-sheet formation resulting from hydrophobic packing, establishment of stabilizing hydrogen bonds, and the right balance of attractive and repulsive electrostatic interactions.

Despite our increased understanding of the peptide self-assembly mechanism gathered from different studies [13,20,23], there still remains much to learn about the design and self-assembly of peptides, more specifically about the relationship between the peptide's primary structure and the resulting morphology of the self-assembled nanostructures [32,37,38]. Taking into account the potential applications of peptide hydrogels originating from an edible/biocompatible source, the aim of this work is to gain insight about the structure-assembly relationship of Peptide OP by studying the impact of the amino acid sequence on the nanostructure's conformation, morphology, and hydrogel formation.

In order to achieve this, we designed a series of OP homologs by using strategic amino acid substitutions (Table 1). Since the amphiphilic character of self-assembling peptides appeared to be a key structural determinant to drive self-assembly, we first synthesized a group of peptides with different ratios of hydrophobic and hydrophilic residues (Table 1, H1–H5). Also, as several studies reported on the implication of electrostatic repulsive and attractive interactions arising from lysine residues in peptide self-assembly [8,15,16,33,38,39], we also prepared homologs that had only the lysine residue substituted by other charged amino acids (Table 1, L1 and L2).

Then, to further study the implication of electrostatic repulsive and attractive interactions, we synthesized a group of peptides with identical amino acids to the milk-derived OP, but with different charge distributions (Table 1, D1–D3). Many physico-chemical conditions trigger and control peptide self-assembly, but we chose to focus on pH in this study, since our previous works showed that the self-assembly of octapeptide is strongly dependent on pH variations [35,36].

Circular dichroism spectropolarimetry (CD) was used to study the secondary structure of the modified peptides at different pH values in order to determine which amino acid substitutions induce or inhibit β-sheet formation and therefore self-assembly. Transmission electron microscopy (TEM) was used to observe the impact of amino acid modifications on nanostructure morphology. Further, the potential to form hydrogels was investigated for all the homologous peptides able to undergo secondary structure transition to β-sheet conformation. Hydrogel formation was triggered by pH variations and

hydrogels were then characterized using visual observations. The overall outcome of this work is to move toward a better understand of the unique gelation properties of naturally derived peptides and to refine even further the molecular detail of the self-assembly process in order to design better materials especially suitable for industrial applications.

## 2. Materials and methods

### 2.1. Materials

All peptides were prepared using standard solid-phase Fmoc strategy and synthesized on Wang resin, except for Peptide D2 that was synthesized on Rink resin. The 2-(1H-benzotriazol1-yl)-1,1,3,3-tetramethyl uranium hexafluorophosphate/1-hydroxy-benzotriazole (HBTU/HOBT) mixture was used as the coupling reagent. The amine group deprotection cycles were achieved using a solution of 20% piperidine in N,N-dimethylformamide(DMF). The resulting resin-bound peptides were cleaved and side-chain deprotected by use of trifluoroacetic acid (TFA)/water ($H_2O$)/1,2-ethane dithiol (EDT)/triisopropylsilane (TIS) (94:2.5:2.5:1). In order to recover the peptides and eliminate impurities, the peptides were triturated 5 times with petroleum ether and then vacuum-dried. All peptides were characterized by HPLC and ESI mass spectrometry.

### 2.2. Circular dichroism (CD) spectropolarimetry

Analyses were performed using a Jasco J-710 instrument (upgraded to a J-715) with 1.08.01 spectral management software using freshly prepared aqueous solutions of peptides with a concentration of 2 mg/mL. The solubilization of peptides was improved by combining the addition of 10% (v/v) of 2,2,2-trifluoroethanol (TFE) with a 20 minute ultrasonic treatment. Spectra were recorded at 22 °C in quartz cylindrical cells with a 0.01 cm path length. Ten scans were collected from 250 to 190 nm with a data pitch of 0.2 nm and a scanning speed of 100 nm/min. For all CD experiments, the pH adjustments were done using NaOH and HCl solutions. Amounts added for pH adjustments were taken into account in the calculation of the final peptide concentration. All CD measurements were duplicated. The resulting data were background-corrected and smoothed.

### 2.3. Transmission electron microscopy

Samples were prepared by rehydrating lyophilized peptides to a concentration of 5 mM and agitating for 1 h. The pH was then adjusted to 10.0 and samples were left to rest for 30 min to allow nanostructure formation at higher peptide concentrations. The peptide solutions were then diluted to a final peptide concentration of 0.50 mM and the pH was readjusted for each solution. 2 µL of each sample was applied to a carbon-coated copper grid and air-dried. The samples were negatively stained with 2 µL of 1% uranyl acetate solution and air-dried. Specimens were examined with a JEM 1230

transmission electron microscope appliance (JEOL, Tokyo, Japan) at 80 kV accelerating voltage. Images were captured with a Gatan digital imaging camera and software (Gatan, Pleasanton, CA).

### 2.4. Hydrogel formation

Peptide solutions were prepared in HPLC nanopure water at a concentration of 1% (10 mg/mL), and then the solutions were shaken for 1 h. Each stock peptide solution was divided into three vials in order to study the hydrogel formation in acidic, neutral, and basic environments. The pH in the vials was adjusted with 1 N and 0.5 N NaOH or HCl to pH 2.0, 6.0, or 10.0. The hydrogels obtained were then characterized by visual observations.

## 3. Results

### 3.1. Conformational characterization of the modified peptides

The ability of the homologs to form β-sheets was assessed by CD over a broad pH range, from pH 2.0 to 12.0 (Figs. 1–3).

#### 3.1.1. Influence of the hydrophilic/hydrophobic ratio

In order to study the effects of varying the ratio of hydrophobic and hydrophilic residues, the N-terminal hydrophobic extremity of Peptide OP was modified. Fig. 1 shows the CD spectra of Peptide OP and homologs H1–H5.

First, two peptides were synthesized and studied: one with leucine residue replaced by a glycine (H1) and one with an additional leucine (H2). For Peptide H1, the CD spectra show a negative minimum around 200 nm, indicating that H1 adopts mostly a random coil conformation at all pH values. These results showed that decreasing hydrophobicity at the N-terminal extremity drastically inhibits β-sheet formation and therefore self-assembly. The CD spectra recorded for Peptide H2 show a negative minimum around 220 nm and a positive maximum around 200 nm; this is typical of β-sheet conformation at every pH value, but particularly for pH 6.0 and 8.0, which show a much more intense signal in neutral and basic environments. These results demonstrate that lengthening the hydrophobic extremity, even by adding one leucine residue, not only triggered β-sheet formation at basic pH values (as for OP), but also triggered β-sheet formation over the entire pH range. Together, results with Peptides
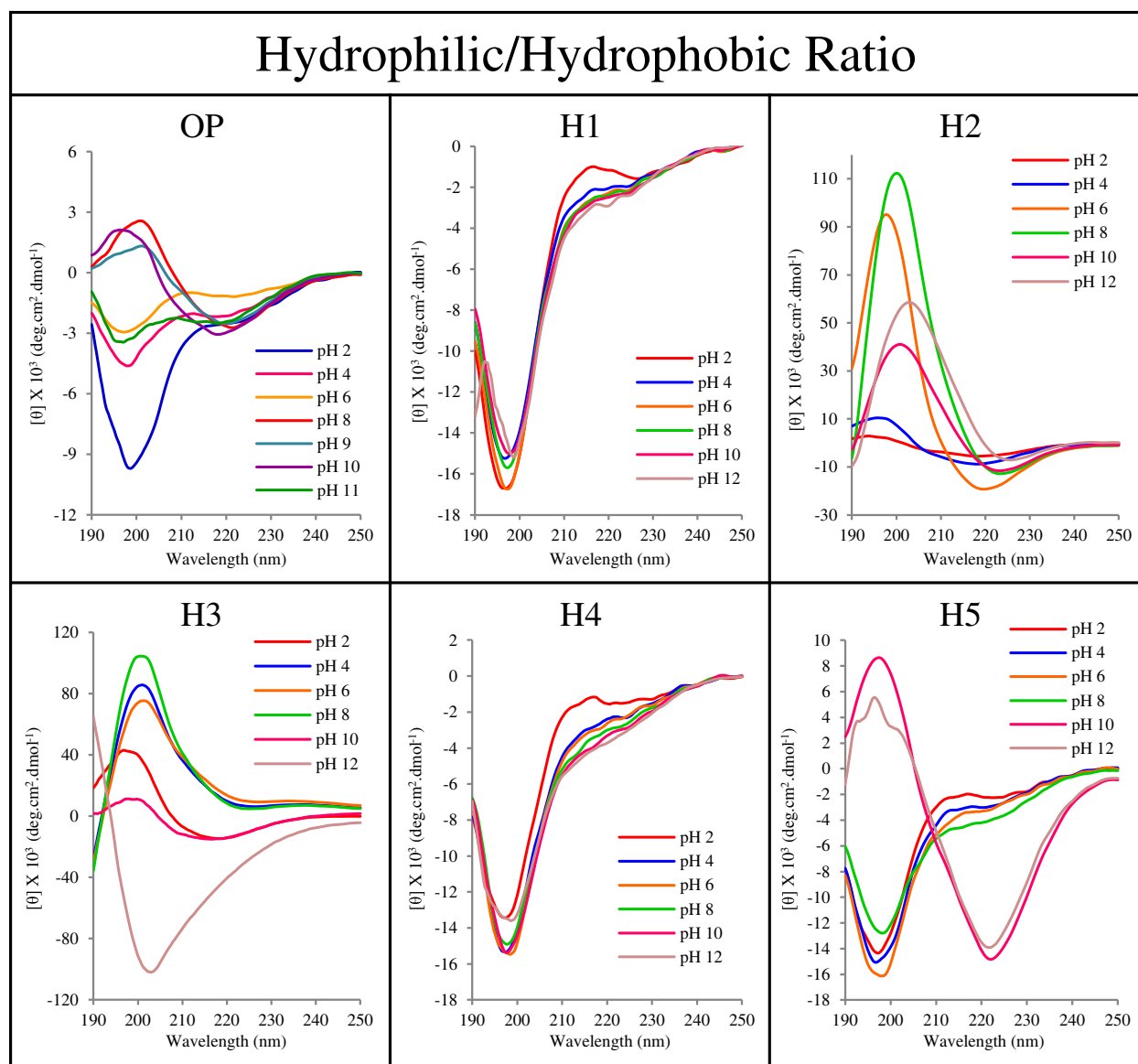


Fig. 1. Circular dichroism spectra of Peptide OP and H1–H5 homologs. Spectra recorded at different pH at a concentration of 2 mg/mL in water with 10% (v/v) of 2,2,2-trifluoroethanol (TFE) at 20 °C.
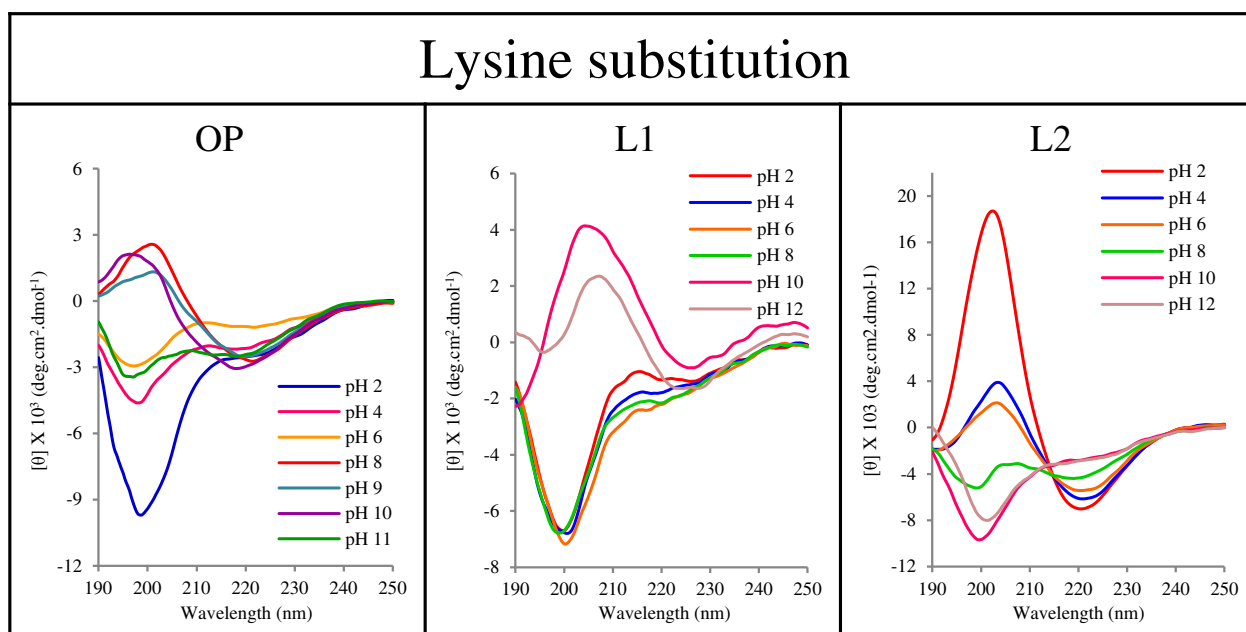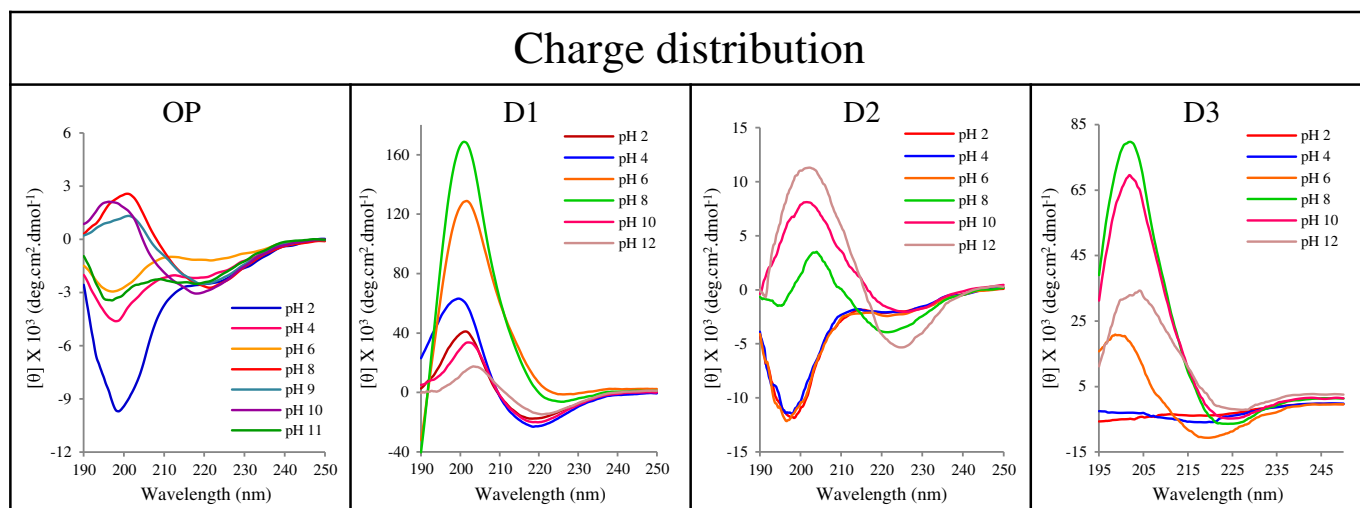
**Fig. 2.** Circular dichroism spectra of Peptide OP and L1 and L2 homologs. Spectra recorded at different pH at a concentration of 2 mg/mL in water with 10% (v/v) of 2,2,2-trifluoroethanol (TFE) at 20 °C.

H1 and H2 demonstrate that hydrophobic interactions are essential to drive self-assembly of Peptide OP, and have a strong impact on the β-sheet self-assembly mechanism. These results also support our previous hypothesis on hydrophobic interactions, which was that they act as driving forces in the self-assembly of Peptide OP through hydrophobic packing of the hydrophobic amino acid side chains, which initiates β-sheet formation [36].

To further study the effect of varying the ratio of hydrophobic and hydrophilic residues of Peptide OP, we first substituted the C-terminal lysine residue with an alanine (H3), and also substituted the methionine by a lysine (H4). As depicted in Fig. 1, the CD spectra of Peptide H3 show a negative minimum around 220 nm and a positive maximum around 200 nm for pH values of pH 2.0 and 10.0. This indicates that Peptide H3 adopts a typical β-sheet conformation and is able to undergo self-assembly in strongly acidic or basic environments.

This result demonstrates again that a slight modification of the amino acid sequence of Peptide OP leads to an important broadening of the pH conditions that trigger self-assembly. For Peptide H3, it is reasonable to invoke the implication of electrostatic interactions in the β-sheet self-assembly mechanism. Indeed, because the hydrophilic C-terminal extremity of the Peptide OP is a lysine, its substitution for an alanine resulted in the loss of the positive charge carried by the lysine side chain, and therefore led to an important decrease of the electrostatic character. As previously mentioned, a decrease in the repulsive electrostatic interactions between neighboring side chains allows peptide units to get closer, improves intermolecular bonding between peptide backbones, and increases β-sheet formation [36].

Changes in H3 spectra are observed for pH values around neutrality, notably between pH 4.0 and 8.0. The negative minimum around 220 nm tends to disappear while the positive maximum around



**Fig. 3.** Circular dichroism spectra of Peptide OP and D1–D3 homologs. Spectra recorded at different pH at a concentration of 2 mg/mL in water with 10% (v/v) of 2,2,2-trifluoroethanol (TFE) at 20 °C.

200 nm increases. These CD spectra could be interpreted as incorporating some β-turn conformation with the β-sheet. However, CD spectroscopy is not an accurate method for β-turn identification especially when mixed with other secondary structures. Nevertheless, CD spectra indicate that Peptide H3 experiences a structural transition at pH values between pH 4.0 and 8.0, but remains in a structured conformation at these pH values. Finally, H3 becomes a random coil at pH 12.0 and over, indicated by a strong negative minimum around 200 nm in the CD spectra. Together, the CD results of Peptide H3 demonstrate that the C-terminal hydrophilic extremity of Peptide OP is not essential to trigger self-assembly and therefore seems to play a less important role in β-sheet self-assembly mechanism than the N-terminal hydrophobic extremity.

For Peptide H4 with an additional terminal lysine in place of the neutral methionine, the CD spectra in Fig. 1 show a single negative minimum around 200 nm at all pH values, indicating that adding a positive charge and increasing the C-terminal hydrophilic extremity provokes a structural transition to random coil conformation, which impedes self-assembly. Adding one lysine residue at the C-terminal extremity increases enough the repulsive electrostatic interactions to disfavor the equilibrium between molecular interactions that drives Peptide OP self-assembly.

Finally, a peptide with a duplication of terminal residues at both ends was synthesized and studied (Fig. 1, H5). The CD spectra of Peptide H5 shows a single negative minimum around 200 nm, indicating that H5 is structureless from pH 2.0 to 8.0. Then, for pH values of 10.0 and higher, changes in the CD spectra are observed with a negative minimum around 220 nm and a positive maximum around 200 nm, indicating that H5 experiences a secondary structure transition to a β-sheet conformation in a basic environment. Interestingly, the CD spectra of Peptide H5 are similar to the CD spectra of Peptide OP as a function of pH, except that the structural transition occurs at pH 8.0 and higher for Peptide OP [35]. It appears that simultaneously adding an additional leucine residue to the hydrophobic extremity and incorporating an additional lysine residue to the hydrophilic end produces the same balance between hydrophobic and electrostatic interactions as the one involved in Peptide OP self-assembly.

The results of both Peptides H4 and H5 demonstrate the necessity of a precise balance between hydrophobic and electrostatic interactions to drive β-sheet self-assembly; one change in the ratio between the number of hydrophobic residues and charged residues may shift the equilibrium toward either self-assembly or complete disassembly [33]. Overall, varying the ratio of hydrophobic to hydrophilic residues at extremities highlights that the correct balance between hydrophobic and electrostatic interactions is a key determinant to drive the β-sheet self-assembly of Peptide OP. This further demonstrates the crucial role that the amino acid sequence plays in the peptide self-assembly process.

### 3.1.2. Influence of electrostatic interactions

CD analyses were also performed to investigate the implications of electrostatic repulsive and attractive interactions arising from the lysine terminal residue in Peptide OP self-assembly (Fig. 2). Two peptides were synthesized with the C-terminal lysine residue substituted by an arginine residue (L1) or by a glutamic acid residue (L2). The CD spectra of Peptide L1 show a single negative minimum around 200 nm for pH values between 2.0 and 8.0. This is typical of random coil conformation. A transition to β-sheet conformation occurs at pH 10.0, indicated by a minimum around 220 nm and a maximum around 200 nm.

The CD spectra as a function of pH for Peptide L1 and Peptide OP are very similar, except that the secondary structure transition experienced by L1 takes place at a more basic environment than for OP, which experiences a secondary structure transition at pH 8.0 [35]. This could be explained by the pK$_a$ value of the arginine side chain (12.5), which is higher than the pK$_a$ value of the lysine side chain (10.5), so that the arginine side chain remains protonated and

stabilizes β-sheet structures at more basic pH values than lysine. These results also demonstrate that the terminal lysine can be replaced in the OP sequence by other positively charged amino acids without disrupting self-assembly. Also, according to the amino acid side chain pK$_a$ value, it is possible to broaden the pH conditions under which Peptide OP self-assembly is triggered.

Moving to a more drastic change, substituting the lysine for a glutamic acid at the C-terminal extremity, the CD spectra of Peptide L2 (Fig. 2) at pH 2.0, 4.0, and 6.0 display typical β-sheet conformation curves, but with a much more intense signal at pH 2.0. At pH 8.0, Peptide L2 units exist in both random coil and β-sheet conformations, as is shown by two negative minima, one around 220 nm and the other around 200 nm in the CD spectrum. The complete structural transition to random coil conformation for L2 occurs at pH 10.0 as shown by a strong minimum around 200 nm. Hence, replacing the lysine residue by a negatively charged glutamic acid results in CD spectra over different pH values very similar to the ones of Peptide OP, except that β-sheet formation is triggered in acidic conditions due to the pK$_a$ of the glutamic acid side chain (4.3). These results further illustrate, remarkably, that electrostatic interactions can be engineered to initiate folding into β-sheet and self-assembly [25].

In order to further study the implications of electrostatic repulsive and attractive interactions, CD analyses were performed on peptides with different charge distributions (Fig. 3, D1–D3). These charge variations were achieved by synthesizing peptides with either the C- or N-terminal extremity protected and with a peptide having the reversed sequence to Peptide OP (D3). Thus, Peptide D1 has its N-terminal extremity acetylated in order to eliminate the positive charge arising from the protonation of the free amino group. The CD spectra of Peptide D1 shows a negative minimum around 220 nm and a positive maximum around 200 nm. This is typical of β-sheet conformation at all pH values, but with a much more intense signal for pH 6.0 and 8.0. It appears that eliminating the N-terminal positive charge on Peptide OP strongly promotes β-sheet formation and allows the expansion of pH conditions in which self-assembly is triggered. This could be because the N-terminal positive charge is situated just next to the hydrophobic end (Leu-Ile-Val) in the Peptide OP sequence. Acetylation avoids interference between electrostatic and hydrophobic interactions and therefore increases the hydrophobic character of the hydrophobic extremity. The results of Peptide D1 again support the idea that hydrophobic interactions have a significant impact on the self-assembly mechanism and act as driving forces in the self-assembly of Peptide OP.

Along the same line, Peptide D2 was synthesized with its C-terminal amidated in order to eliminate the negative charge arising from deprotonation of the free carboxyl group. As seen in Fig. 3, Peptide D2 is structureless at pH 2.0, 4.0, and 6.0, as is indicated in the CD spectra by a single negative minimum around 200 nm. However, D2 exists in a β-sheet conformation at pH 8.0, 10.0, and 12.0, as shown by typical minimum around 220 nm and maximum around 200 nm. It is noteworthy that Peptide D2 shows similar CD spectra to Peptide OP and experiences exactly the same structural transition as a function of pH. It seems that the negative charge arising from the C-terminal extremity does not have a noticeable involvement in the self-assembly mechanism of Peptide OP. This result points out the possibility of adding different groups at the C-terminal position without altering the self-assembly process.

Finally, Peptide D3 was synthesized with the reverse amino acid sequence to Peptide OP, which means that the hydrophilic extremity (Lys) is situated at the N-terminal end and the hydrophobic extremity (Leu-Ile-Val) is at the C-terminal end. Results show that Peptide D3 adopts a stable β-sheet conformation over the entire pH range studied, from pH 2.0 to 12.0, as seen in the CD spectra of Fig. 3. Moving the hydrophobic extremity (Leu-Ile-Val) from the positively charged N-terminal over to the C-terminal increased the hydrophobicity at that extremity, and this favored β-sheet assembly. This result further supports the idea that increasing the hydrophobic interactions

strongly promotes β-sheet formation and enhances self-assembly over a wider pH range.

Overall, these results highlight that changes in charge distribution modify the equilibrium between molecular interactions that are involved in the self-assembly mechanism; therefore charge distribution is also a key determinant driving β-sheet self-assembly of Peptide OP.

### 3.2. Impact of amino acid substitutions on the morphology of nanostructures

Micrographs of nanostructures formed at pH 10.0 by the original peptide and its analogs were captured by transmission electron microscopy (TEM) (Fig. 4). Nanostructures were studied in a basic environment, since previous works showed that Peptide OP is in a β-sheet conformation in the pH range of pH 9.0–11.0 [35] and forms a fiber network at pH 9.0 and 10.0 [36]. Moreover, all modified peptides have a β-sheet conformation at pH 10.0, except Peptides H1, H4 and L2. For L2, studies were conducted at pH 2.0 because the glutamic acid side chain ionization level triggers β-sheet formation only in an acidic environment.

Nanostructures formed by peptides with a different ratio of hydrophobic and hydrophilic residues are reported in Fig. 4B–F. The electron micrograph of Peptide H1 (B), with a less hydrophobic N-terminal end, shows both well-defined nanofibers a few nanometers wide and

approximately one micron long, and small nanospheres only a few nanometers in diameter. Peptide H2 (C), with additional hydrophobicity at the N-terminal position, forms mostly well-defined entangled nanofibers a few nanometers wide and approximately one micron long, with a more linear morphology than Peptide H1 fibers. The TEM picture of Peptide H3 (D), with the reduced hydrophilicity at the C-terminal end, displays a homogenous fibrous aggregate with fewer clearly defined fibers. Peptide H4, with increased hydrophilicity at the C-terminal position, forms very similar nanostructures to Peptide H1, mostly well-defined nanofibers a few nanometers wide and approximately one micron long, as well as some nanospheres with diameters of only a few nanometers. The micrograph of H5 (F), with longer hydrophobic and hydrophilic extremities, forms a fibrous aggregate with some well-defined fibers a few nanometers wide by approximately one micron long. It exhibits a stiffer morphology, similar to those observed for Peptide H2.

These TEM results first demonstrate that changing the ratio of hydrophobic and hydrophilic residues leads to the formation of quite different nanostructures. Indeed, nearly identical peptides, differing by only one amino acid, self-assemble into significantly different fiber morphologies [38]. Also, Peptide H2, with an additional leucine at the hydrophobic extremity, forms the best-defined fibers and also forms many more fibers than the peptides with a different ratio of hydrophobic to hydrophilic residues. This result demonstrates once
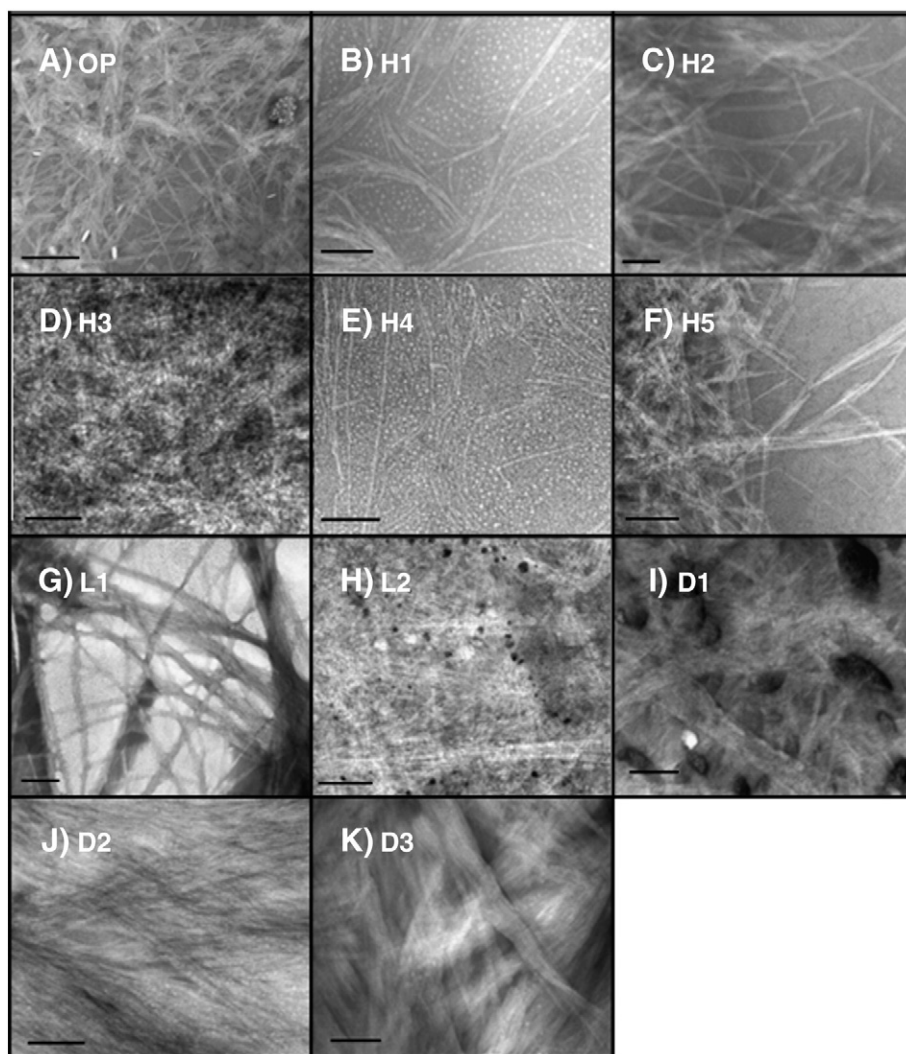


**Fig. 4.** Electron micrograph of OP and all analogs obtained from pH 10 aqueous solutions, except for peptide L2 (H) prepared from a pH 2 solution (see text for details). The bar represents 200 nm.

more that increasing hydrophobic interactions at the N-terminal extremity highly promotes peptide self-assembly into nanofibers. This observation reinforces the idea that hydrophobic packing of leucine side chains is a primary thermodynamic driving force for peptide self-assembly in water [33].

Fig. 4 shows nanostructures formed by peptides with the C-terminal lysine residue substituted by other charged amino acids. The Peptide L1 (G; Lys to Arg) electron micrograph displays well-defined nanofibers a few nanometers width by approximately one micron long entangled together with a rigid and linear morphology. Peptide L2 with a glutamic acid at the C-terminal (H) does not form well-defined nanostructures, but rather aggregates and has very few nanofibers. Interestingly, L2 adopts a β-sheet conformation at the pH used for TEM studies (pH 2 in this case), demonstrating that conformational bias is not sufficient on its own for driving nanofiber formation. Fig. 4 also supports the idea that Peptides L1 and L2, which exhibit a β-sheet CD spectrum at the pH condition corresponding to TEM analyses (pH 10 and 2) form notably different nanostructures. These results point again to the conclusion that peptides with nearly identical amino acid sequences, and that adopt the same secondary structure, can self-assemble into significantly different nanostructures. This further highlights the delicate balance that exists between specific side-chain interactions, as some single-point mutations have a dramatic effect on the aggregation of the peptide, electrostatic interactions, and main-chain H-bonds involved in the formation of fibrils [24].

The nanostructures formed by peptides with the same amino acid content but with a different charge distribution than Peptide OP (D1–D3) are reported in Fig. 4. The TEM shows that Peptide D1 (I), without an N-terminal positive charge, forms a rather dense entangled fibrous network with some pores. The morphology appears more structured than random aggregates with some defined fibers. On the other hand, the Peptide D2 electron micrograph (J) displays many long and well-defined nanofibers a few nanometers wide and one micron long, entangled very closely into a much more compact network. Peptide D3 (K), with the reversed sequence, forms fibrous and ribbon-like nanostructures which exhibit a flat and laminar morphology not observed in the other analogs. It is worth noting that Peptides D1, D2, and D3 all exhibit a β-sheet conformation at the pH conditions used for TEM analyses, even though the sheet content varies significantly.

These TEM results demonstrate that peptides with exactly the same amino acid content but with a different charge distribution can assemble via β-sheet self-assembly. However, the resulting nanostructure they formed bears some differences. This further illustrates that a slight change in the electrostatic interactions due to a different charge distribution plays a significant role in determining the nanostructures formed by analogous peptides [31]. Overall, TEM analyses on modified peptides highlight that primary structure substitutions and changes in the charge distribution lead to important changes in nanostructure morphology. Nevertheless, the nanostructures usually correlate with the conformational preferences of the peptides.

### 3.3. Hydrogel formation of modified peptides

The ability to form hydrogels for Peptide OP and its analogs was studied in acidic (pH 2.0), neutral (pH 6.0) and basic (pH 10.0) pH environments (Figs. 5 and 6). First, as expected, analogs H1 and H4, which are structureless at all pH values, are not able to form hydrogel. Results shown in Fig. 5 illustrates that Peptide H2 forms a self-supporting hydrogel in an acidic and neutral environment, as expected from CD results indicating that H2 adopts a β-sheet conformation in these pH conditions (Fig. 1). However, no gel is formed at pH 10, even if H2 is partially in a β-sheet conformation and forms a network of entangled well-defined nanofibers (Fig. 4C). This could be explained by the important implication of peptide concentration in β-sheet self-assembly of Peptide OP, as we previously described [36]. Indeed, due to technical restrictions, TEM analysis were made
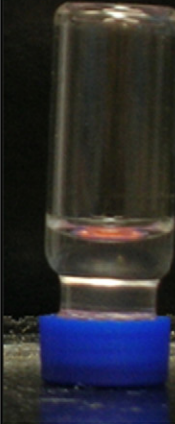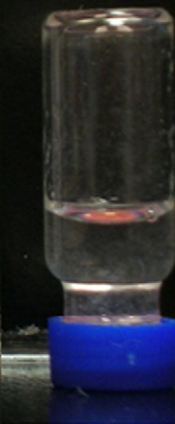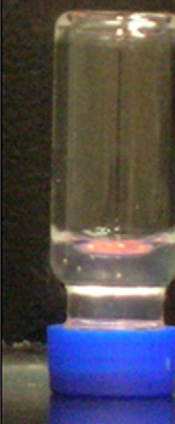
| Peptide | Acidic pH | Neutral pH | Basic pH |
|---------|-----------|------------|----------|
| OP | - | - | G |
| H1 | - | - | - |
| H2 | G | G | - |
| H3 | G | G | G |
| H4 | - | - | - |
| H5 | - | - | G |
| L1 | - | - | G |
| L2 | G | G | - |
| D1 | - | G | G |
| D2 | - | - | G |
| D3 | G | G | G |

**Fig. 5.** Hydrogel formation ability of Peptide OP and its analogs. The G indicates that gel is formed, and – indicates that no gel is formed.

on very dilute samples, while gel formation was studied at a higher peptide concentrations, as the critical peptide concentration for hydrogel formation of OP is 2.0 mg/mL. This result highlights that TEM results, although useful, cannot be used solely to establish links between gel formation and morphology at the nanoscale level, due to the dilution effect.

Peptide H3 forms a weak gel at acidic pH, but forms a self-supporting hydrogel at neutral and basic pH. These results are consistent with CD results (Fig. 1) showing that Peptide H3 adopts a β-sheet conformation at pH values between pH 2.0 and 10.0, with a significant proportion of the sheet at pH values around neutrality. For Peptide H5, hydrogel formation occurs only in basic conditions, which corresponds to the pH range where the peptide is strongly folded into a β-sheet. Peptide L1 undergoes hydrogelation only in a basic environment, which is in agreement with CD results indicating that L1 adopts a β-sheet conformation at basic pH values. On the other hand, Peptide L2 forms weak hydrogels at acidic and neutral pH and no gel is formed at basic pH values. Those results were expected as CD results demonstrated that L2 is strongly folded into a β-sheet from pH 2.0 to 6.0 and that a structural transition to random coil conformation begins at pH 8.0 and is completed at higher pH values. However, even if the CD results for Peptides L1 and L2 revealed that the C-terminal lysine residue can be replaced both by positively and negatively charged amino acids without disrupting much of the β-sheet conformation, it appeared that lysine substitution by another positively charged residue leads to a better balance between attractive and repulsive electrostatic interactions and improves the formation of a self-supporting hydrogel.

Peptide D1 forms self-supporting hydrogels in neutral and basic environments, as expected based on CD results displaying typical β-sheet curves at those pHs. A hydrogel was also expected at acidic pH, but formed rather slowly after several days. Nonetheless, among all OP homologs, D1 clearly has the best propensity for β-sheet self-assembly and for hydrogel formation. Thus, it seems that eliminating the N-terminal positive charge on Peptide OP leads to the optimal balance between electrostatic and hydrophobic interactions and hydrogen bonding, maximizes β-sheet self-assembly, and therefore drastically improves hydrogel formation. For Peptide D2, with the C-terminal extremity blocked, no gel is formed at acidic and neutral pH values, but a self-supporting hydrogel is formed in basic conditions. Those results are consistent with both CD results showing that D2 adopts a β-sheet conformation in a basic environment. Peptide D3 forms self-supporting hydrogels in acidic, neutral and basic pH values, but at a much slower rate than D1 (24 h). These results are also consistent with CD results as D3 adopts a β-sheet conformation over the entire pH range, but, with much more intense signal for pH values of pH of 6.0 and higher.

| Peptide | Acidic pH | Neutral pH | Basic pH |
|---------|-----------|------------|----------|
| H2 | 1 hr | Instantly | No gel |
| L1 | No gel | No gel | Instantly |
| D1 | No gel | Instantly | Instantly |

Fig. 6. Hydrogel formation potential of different OP homologs (H2, L1, and D1) used in this study at a peptide concentration of 1% (10 mg/mL) in acidic (pH 2.0), neutral (pH 6.0), and basic (pH 10.0) environment.

Overall, the investigation of hydrogel formation first demonstrates that slightly modifying the sequence of Peptide OP by replacing one or two amino acids leads to an important diversification of the pH conditions in which hydrogel formation occurs. Indeed, Peptide OP can form hydrogels only in basic conditions, while many analogs undergo hydrogelation either at acidic, neutral, or basic pH values, depending on the amino acid substitutions (Figs. 5 and 6). Additionally, Fig. 6 highlights that simple modification on the amino acid sequence of Peptide OP also substantially impacts hydrogel formation rates. Indeed, some analogs can form hydrogels instantly, whereas others will form hydrogels in 24 h under similar conditions. Also, it is worth noting that hydrogel formation occurs only when analogs adopt a sufficiently strong β-sheet conformation. Hence, the gelation appeared to be fully dependent on the folded state of the peptide, implying a direct relationship between β-sheet formation (measured by CD spectropolarimetry) and the evolution of network structure [25].

## 4. Conclusion

Overall, the present study highlights some key factors in amino acid sequences that have a significant impact on β-sheet self-assembly, nanostructure morphology, and hydrogel formation. We have confirmed that a hydrophobic extremity is essential to drive the self-assembly of Peptide OP and that hydrophobic interactions act as a driving force that initiates β-sheet formation and promotes peptide self-assembly.

Secondly, this study has shown that electrostatic interactions arising from the hydrophilic extremity (C-terminal) of Peptide OP contribute considerably to the precise equilibrium between the hydrophobic and electrostatic interactions required to drive β-sheet self-assembly. Moreover, it highlights that C-terminal lysine can be replaced either by a positively or negatively charged amino acid without inhibiting the β-sheet conformation. However, only the charged residue (arginine) leads to a better balance between attractive and repulsive electrostatic interactions and highly improved gelation rates.

Thirdly, the results identified that among all the structural modifications achieved, the elimination of the N-terminal positive charge in Peptide OP (D1) leads to an optimal balance between favorable and unfavorable molecular interactions. This modification also maximizes the β-sheet self-assembly and therefore drastically improves hydrogel formation rate and stability, at least under neutral and basic conditions.

Finally, the data reported in this study demonstrate that it is possible to engineer the properties of peptide-based hydrogels and to diversify the physicochemical conditions in which β-sheet self-assembly and hydrogel formation are triggered, to generate nanostructures exhibiting very different morphologies. Hence, the work reported here sheds light on key molecular features involved in the formation of useful hydrogels defined at the nanoscale. Further, its opens doors for the identification of novel peptide-based hydrogels derived from natural edible materials. Considering the various possible uses for these self-assembling peptides from food proteins, we are currently investigating the biocompatibility of designed hydrogels and studying gelation kinetics in more detail.

## Acknowledgments

## Appendix A. Supplementary data

Supplementary data to this article can be found online at doi:10.1016/j.bpc.2011.12.005.

## References

[1] J.-M. Lehn, Supramolecular Chemistry — Concepts and Perspectives, VCH, Weinheim, 1995.
[2] N. Sakai, J. Mareda, S. Matile, Artificial ß-barrels, Accounts of Chemical Research 41 (2008) 1354–1365.
[3] N.C. Seeman, Nanomaterials based on DNA, Annual Review of Biochemistry 79 (2010) 65–87.
[4] S.I. Stupp, Self-assembly and biomaterials, Nanoletters 10 (2010) 4783–4786.
[5] D. Berti, Self assembly of biologically inspired amphiphiles, Current Opinion in Colloid & Interface Science 11 (2006) 74–78.
[6] T.C. Holmes, S. De Lacalle, X. Su, G. Liu, A. Rich, S. Zhang, Extensive neurite outgrowth and active synapse formation on self-assembling peptide scaffolds, Proceedings of the National Academy of Sciences of the United States of America 97 (2000) 6728–6733.
[7] J. Kirkham, A. Firth, D. Vernals, N. Boden, C. Robinson, R.C. Shore, S.J. Brookes, A. Aggeli, Self-assembling peptide scaffolds promote enamel remineralization, Journal of Dental Research 86 (2007) 426–430.
[8] D. Salick, J.K. Kretsinger, D.J. Pochan, J.P. Schneider, Inherent antibacterial activity of a peptide-based β-hairpin hydrogel, Journal of the American Chemical Society 129 (2007) 14793–14799.
[9] J. Kretsinger, L.A. Haines, B. Ozbas, D.J. Pochan, J.P. Schneider, Cytocompatibility of self-assembled β-hairpin peptide hydrogel surfaces, Biomaterials 26 (2005) 5177–5186.
[10] R.J. Brea, C. Reiriz, J.R. Granja, Towards functional bionanomaterials based on self-assembling cyclic peptide nanotubes, Chemical Society Reviews 39 (2010) 1448–1456.
[11] L.W. Chow, R. Bitton, M.J. Webber, D. Carvajal, K.R. Shull, A.K. Sharma, S.I. Stupp, A bioactive self-assembled membrane to promote angiogenesis, Biomaterials 32 (2011) 1574–1582.
[12] H. Cui, M.J. Webber, S.I. Stupp, Self-assembly of peptide amphiphiles: from molecules to nanostructures to biomaterials, Biopolymers: Peptide Science 94 (2010) 1–18.
[13] R.V. Ulijn, A.M. Smith, Designing peptide based nanomaterials, Chemical Society Reviews 37 (2008) 664–675.
[14] A. Aggeli, I.A. Nyrkova, M. Bell, R. Harding, L. Carrick, T.C.B. Mcleish, A.N. Semenov, N. Boden, Hierarchical self-assembly of chiral rod-like molecules as a model for peptide β-sheet tapes, ribbons, fibrils, and fibers, Proceedings of the National Academy of Sciences of the United States of America 98 (2001) 11857–11862.
[15] L. Haines-Butterick, K. Rajagopal, M. Branco, D.A. Salick, R. Rughani, M. Pilarz, M. Lamm, D.J. Pochan, J.P. Schneider, Controlling hydrogelation kinetics by peptide design for three-dimensional encapsulation and injectable delivery of cells, Proceedings of the National Academy of Sciences of the United States of America 104 (2007) 7791–7796.
[16] K. Rajagopal, B. Ozbas, D.J. Pochan, J.P. Schneider, Probing the importance of lateral hydrophobic association in self-assembling peptide hydrogelators, European Biophysics Journal 35 (2006) 162–169.
[17] J.P. Schneider, D.J. Pochan, B. Ozbas, K. Rajagopal, L. Pakstis, J. Kretsinger, Responsive hydrogels from the intramolecular folding and self-assembly of a designed peptide, Journal of the American Chemical Society 124 (2002) 15030–15037.
[18] G. Tuchscherer, A. Chandravarkar, M.-J. Camus, J. Bérard, K. Murat, A. Schmid, R. Mimna, H.A. Lashuel, M. Mutter, Switch-peptides as folding precursors in self-assembling peptides and amyloid fibrillogenesis, Biopolymers 88 (2007) 239–252.
[19] C. Wang, L. Huang, L. Wang, Y. Hong, Y. Sha, One-dimensional self-assembly of a rational designed β-structure peptide, Biopolymers 86 (2007) 23–31.
[20] M. Reches, E. Gazit, Molecular self-assembly of peptide nanostructures: mechanism of association and potential uses, Current Nanoscience 2 (2006) 105–111.
[21] D.T. Bong, T.D. Clark, J.R. Granja, M.R. Ghadiri, Self-assembling organic nanotubes, Angewandte Chemie International Edition 40 (2001) 988–1011.
[22] A. Aggeli, M. Bell, N. Boden, J.N. Keen, P.F. Knowles, T.C. McLeish, M. Pitkeathly, S.E. Radford, Responsive gels formed by the spontaneous self-assembly of peptides into polymeric β-sheet tapes, Nature 386 (1997) 259–262.
[23] R. Fairman, K.S. Åkerfeldt, Peptides as novel smart materials, Current Opinion in Structural Biology 15 (2005) 453–463.
[24] M. López de la Paz, K. Goldie, J. Zurdo, E. Lacroix, C.M. Dobson, A. Hoenger, L. Serrano, De novo designed peptide-based amyloids fibrils, Proceedings of the National Academy of Sciences of the United States of America 99 (2002) 16052–16057.
[25] C. Veerman, K. Rajagopal, C.S. Palla, D.J. Pochan, J.P. Schneider, E.M. Furst, Gelation kinetics of β-hairpin peptide hydrogel networks, Macromolecules 39 (2006) 6608–6614.
[26] J. Kopeček, J.Y. Yang, Peptide-directed self-assembly of hydrogels, Acta Biomaterialia 5 (2009) 805–816.
[27] E.L. Bakota, Y. Wang, R. Farhad, R. Danesh, J.D. Hartgerink, Injectable multidomain peptide nanofiber hydrogel as a delivery agent for stem cell secretome, Biomacromology 12 (2011) 1651–1657.

[28] M.J. Webber, J.A. Kessler, S.I. Stupp, Emerging peptide nanomedicine to regenerate tissues and organs, Journal of Internal Medicine 267 (2010) 71–88.

[29] M.J. Webber, J. Tongers, M.-A. Renault, J.G. Roncalli, D.W. Losordo, S.I. Stupp, Development of bioactive peptide amphiphiles for therapeutic cell delivery, Acta Biomaterialia 6 (2010) 3–11.

[30] A. Aggeli, M. Bell, L.M. Carrick, C.W.G. Fishwick, R. Harding, P.J. Mawer, S.E. Radford, A.E. Strong, N. Boden, pH as trigger of peptide β-sheet self-assembly and reversible switching between nematic and isotropic phases, Journal of the American Chemical Society 125 (2003) 9619–9628.

[31] Y. Hong, R. Legge, S. Zhang, P. Chen, Effect of amino acid sequence and pH on nanofiber formation of self-assembling peptides EAK16-II and EAK16-IV, Biomacromology 4 (2003) 1433–1442.

[32] L.M. Carrick, A. Aggeli, N. Boden, J. Fisher, E. Ingham, T.A. Waigh, Effect of ionic strength on the self-assembly, morphology and gelation of pH responsive β-sheet tape-forming peptides, Tetrahedron 63 (2007) 7457–7467.

[33] H. Dong, S.E. Paramonov, L. Aulisa, E.L. Bakota, J.D. Hartgerink, Self-assembly of multidomain peptides: balancing molecular frustration controls conformation and nanostructures, Journal of the American Chemical Society 129 (2007) 12468–12472.

[34] Z. Ye, H. Zhang, H. Luo, S. Wang, Q. Zhou, X. Du, C. Tang, L. Chen, J. Liu, Y.-K. Shi, E.-Y. Zhang, R. Ellis-Behnke, X. Zhao, Temperature and pH effects on biophysical and morphological properties of self-assembling peptide RADA 16-I, Journal of Peptide Science 14 (2008) 152–162.

[35] Y. Pouliot, M.-M. Guy, M. Tremblay, A.-C. Gaonac'h, B.P. Chay Pak Ting, S.F. Gauthier, N. Voyer, Isolation and characterization of an aggregating peptide from a tryptic hydrolysate of whey proteins, Journal of Agricultural and Food Chemistry 57 (2009) 3760–3764.

[36] M.-M. Guy, M. Tremblay, N. Voyer, S.F. Gauthier, Y. Pouliot, Formation of nanofibers and hydrogels from a milk-derived peptide, Journal of Agricultural and Food Chemistry 59 (2011) 720–726.

[37] G. Colombo, P. Soto, E. Gazit, Peptide self-assembly at the nanoscale: a challenging target for computational and experimental biotechnology, Trends Biotechnology 25 (2007) 211–218.

[38] M.S. Lamm, K. Rajagopal, J.P. Schneider, D.J. Pochan, Laminated morphology of nontwisting β-sheet fribrils constructed via peptide self-assembly, Journal of the American Chemical Society 127 (2005) 16692–16700.

[39] K. Rajangam, M.S. Arnold, M.A. Rocco, S.I. Stupp, Peptide amphiphile nanostructure–heparin interactions and their relationship to bioactivity, Biomaterials 29 (2008) 3298–3305.